Comparison of Lattice Search Techniques for Nonlinear Precoding

Georgios K. Psaltopoulos, Michael Joham, and Wolfgang Utschick
Institute for Circuit Theory and Signal Processing
Munich University of Technology, 80290 Munich, Germany
E-Mail: {geps,mijo,wout}@nws.ei.tum.de

***Abstract*— We introduce a new theoretical framework which comprises linear precoding, *Tomlinson-Harashima precoding* (THP), and *vector precoding* (VP). Whereas linear precoding generates the transmit signal by linearly transforming the data signal, THP and VP linearly transform the superposition of the data signal and a signal obtained by a search in a lattice. We observe that THP is constrained VP, i.e., the search in the lattice is constrained. Moreover, we are able to develop a new precoding scheme, *scaled vector precoding* (SVP), whose diversity order lies between the diversity orders of THP and VP. By including lattice reduction in SVP, we end up with a generalization of Babai's nearest-plane algorithm. Our simulations reveal that lattice reduction and also the new SVP are advantageous for the zero-forcing variants of nonlinear precoding. However, the improvement of THP based on the minimum mean square error criterion by lattice reduction and/or SVP is modest.**

I. Introduction

In the broadcast setup, one transmitter serves several non-cooperative receivers, i.e., no receiver has access to the received signals of the other receivers. Therefore, the data signals for the different receivers have to be processed prior to transmission such that the channel acts like an equalizer, i.e., precoding has to be employed.

The transmit signal of linear precoding results from a linear transformation of the data signal (see [1] and the references therein). To avoid interference between the user's data streams, the transmit filters of linear precoding have to lie in a subspace (nearly) orthogonal to the channels of the other users. Consequently, little degrees of freedom are available to exploit the diversity offered by the channel with multiple transmit antennas and the diversity order of linear precoding is poor, that is, the slope of the error curves is small for high *signal-to-noise ratio* (SNR).

THP, initially proposed for dispersive single input single output systems (e.g., [2]), was adopted to systems with a centralized transmitter and several decentralized non-cooperative users in [3], [4], [5]. *Zero-forcing* (ZF) THP is very popular [3], [4], [6], [7], [8], [9], [10], where the interference between the user's data streams is perfectly suppressed by applying modulo operations in the feedback loop at the transmitter and to the received signals. However, THP based on the *minimum mean square error* (MMSE) criterion is clearly superior to ZF-THP [5]. In [11], an efficient algorithm for the THP filter computation was proposed with a complexity close to that of linear precoding. THP has a low complexity and substantially outperforms linear precoding, but it also suffers from a poor diversity order, because the transmit filter applied to the data signal of the user to be precoded last lies in the same restricted subspace as for linear precoding.

Like THP, VP exploits the degrees of freedom available due to the receivers' modulo operators [12]. VP linearly transforms the superposition of the data signal and a *perturbation signal*. The interference is completely suppressed by ZF-VP, where the linear transformation is the channel pseudo inverse and the perturbation signal is chosen to minimize the unscaled transmit power [12], [9], [13]. Contrary, MMSE-VP, which was derived in [14] (see also [15] for a suboptimal solution), applies a regularized pseudo inverse and the pertubation signal is found by minimizing the *mean square error* (MSE). For any type of VP, the perturbation signal is found via a closest-point search in a lattice (e.g., [12], [14]). Note that such a search is NP-hard [16, Section 5.3]. Consequently, the complexity of VP is prohibitive. Any type of VP is superior to the respective type of THP, e.g., ZF-VP is superior to ZF-THP. Interestingly, MMSE-THP outperforms ZF-VP for realistic SNR values (see [14]) although the complexity of THP for finding a transmit vector from one data vector is only quadratic (as for linear precoding). However, MMSE-THP is clearly inferior to MMSE-VP and no precoding technique is available up to now which offers a complexity-performance trade-off between the two extreme cases THP and VP.

Windpassinger *et al.* [13] suggested to replace the full closest-point search of ZF-VP with the *nearest-plane approximation* of Babai [17], whose approximate solution is found at a complexity similar to that of THP but with full diversity order and a performance close to that of ZF-VP. The approximate solution of [13] requires the use of the *Lenstra, Lenstra, Lovász* (LLL) lattice basis reduction algorithm, which has quartic complexity [16, Section 5.3]. The application of lattice reduction has not been considered for MMSE-VP yet.

The contributions of this paper are as follows. We introduce a new theoretical framework comprising THP and VP which we review in Section III and IV, respectively. Based on this framework, we observe that THP is constrained VP, i.e., the search in the lattice is constrained. Inspired by [9], we develop a new precoding scheme in Section V, which we call *scaled vector precoding* (SVP), whose diversity order lies between the diversity orders of THP and VP. By including lattice reduction in SVP, we end up with a generalization of the nearest-plane

algorithm in Section VI. Our simulations in Section VII reveal that lattice reduction and also the new SVP are advantageous for the zero-forcing variants of nonlinear precoding. However, the improvement of THP based on the minimum mean square error criterion by lattice reduction and/or SVP is modest.

Notation: Throughout the paper, we denote vectors and matrices by lower and upper case bold letters, respectively. We use $\mathrm{E}[\bullet]$, $(\bullet)^{\mathrm{T}}$, $(\bullet)^{\mathrm{H}}$, $\mathrm{tr}(\bullet)$, '$\otimes$', $\Re(\bullet)$, and $\Im(\bullet)$ for expectation, transposition, conjugate transposition, the trace of a matrix, the Kronecker product, the real part, and the imaginary part, respectively. The $N \times N$ identity matrix is $\boldsymbol{I}_N$. We refer to the imaginary unit as j.

II. System Model

We consider the *Multiple Input Multiple Output* (MIMO) broadcast system with B users illustrated in Fig. 1 where n is the time index. At the base station, $N_{\mathrm{a}} \geq B$ transmit antennas are deployed. Each user has a single receive antenna and is assigned a data stream. The data signals $s_i[n], i = 1, \ldots, B$, are independent complex valued baseband signals and take values from a signal constellation $\mathbb{A}$. The signal vector $\boldsymbol{s}[n] = [s_1[n], \ldots, s_B[n]]^{\mathrm{T}}$ is precoded at the transmitter and the resulting output signal $\boldsymbol{y}[n]$ is transmitted over a flat fading MIMO channel $\boldsymbol{H} \in \mathbb{C}^{B \times N_{\mathrm{a}}}$ with tap-gain $[\boldsymbol{H}]_{j,i}$ from transmit antenna i to receive antenna j. The signal of interest is perturbed at the receiver by the additive zero-mean complex Gaussian noise vector $\boldsymbol{\eta}[n]$ with covariance matrix $\boldsymbol{\Phi}_{\eta\eta} = \sigma_\eta^2 \boldsymbol{I}_B$, leading to the observation

$$\boldsymbol{x}[n] = \boldsymbol{H}\boldsymbol{y}[n] + \boldsymbol{\eta}[n]. \tag{1}$$

The receive processing is restricted to a scaled identity matrix since the receivers are non-cooperative. We consider the transmission of a block of vectors $\boldsymbol{y}[n]$ of length N_{B}, over which the channel $\boldsymbol{H}$ is assumed to be constant and perfectly known at the transmitter.

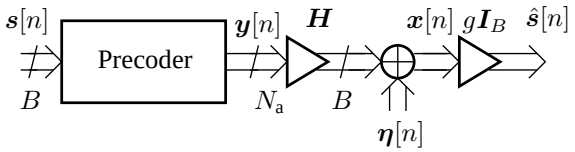

Fig. 1. Transmit Processing Reference Model

III. Tomlinson-Harashima Precoding

We begin by reviewing the principle of THP for frequency flat MIMO channels [11]. Fig. 2 depicts the reference model. The modulo operator is defined element-wise:

$$\mathrm{M}(x) = x - \left\lfloor \frac{\Re(x)}{\tau} + \frac{1}{2} \right\rfloor \tau - \mathrm{j} \left\lfloor \frac{\Im(x)}{\tau} + \frac{1}{2} \right\rfloor \tau.$$

where $\lfloor \bullet \rfloor$ denotes the floor operation which gives the largest integer smaller than or equal to the argument. So, the modulo operator $\mathrm{M}(\bullet)$ maps the real and imaginary part of its argument elementwise to the interval $[-\tau/2, \tau/2)$ by adding integer multiples of τ [11]. The constant τ has to be chosen such that $\mathrm{M}(x) = x, \forall x \in \mathbb{A}$. We see that the modulo operator $\mathrm{M}(\bullet)$ can be substituted with the addition of a perturbation vector $\boldsymbol{\alpha}[n] \in \tau\mathbb{Z}^B + \mathrm{j}\,\tau\mathbb{Z}^B$. This addition can be shifted outside the loop. The resulting linear representation without the modulo operators is depicted in Fig. 3.[1] MMSE-THP

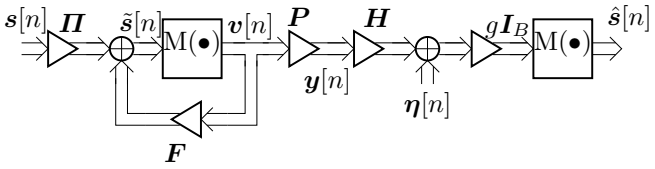

Fig. 2. Block Diagram for Tomlinson-Harashima Precoding.

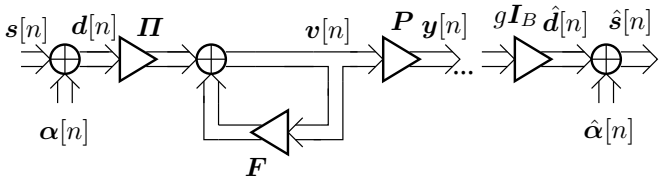

Fig. 3. Equivalent Linear Representation without the Modulo Operators.

tries to minimize the MSE of $\hat{\boldsymbol{d}}[n]$ with respect to $\boldsymbol{d}[n]$, i.e., the variance of the error signal $\boldsymbol{\varepsilon}[n] = \boldsymbol{d}[n] - \hat{\boldsymbol{d}}[n]$. The backward filter $\boldsymbol{F}$ has a lower triangular structure with zero main diagonal, since only already precoded symbols can be fed back. The permutation matrix

$$\boldsymbol{\Pi} = \sum_{i=1}^{B} \boldsymbol{e}_i \boldsymbol{e}_{k_i}^{\mathrm{T}} \tag{2}$$

reorders the elements of $\boldsymbol{s}[n]$ according to the precoding order $\mathcal{O} = (k_1, \ldots, k_B)$. The precoding order $\mathcal{O}$ is part of the optimization. Note that $\boldsymbol{\Pi}$ is unitary, i.e., $\boldsymbol{\Pi}^{-1} = \boldsymbol{\Pi}^{\mathrm{H}}$. We assume that the elements of $\boldsymbol{v}[n]$ are uncorrelated and their covariance matrix is

$$\boldsymbol{\Phi}_{vv} = \mathrm{diag}(\sigma_{v_1}^2, \ldots \sigma_{v_B}^2)$$

where $\sigma_{v_1}^2 = \sigma_s^2$ and $\sigma_{v_i}^2 = \tau^2/6$ for $i = 2, \ldots, B$ [11]. The MSE can be written as

$$\phi = \mathrm{E}\left[\|\boldsymbol{\varepsilon}\|_2^2 \right] = \mathrm{tr}(\boldsymbol{\Phi}_{\varepsilon\varepsilon}), \tag{3}$$

where $\boldsymbol{\Phi}_{\varepsilon\varepsilon}$ is the covariance matrix of $\boldsymbol{\varepsilon}[n]$ as defined in [11]. The transmit power is constrained to be E_{tr}. The optimization problem reads as

$$\{\boldsymbol{F}_{\mathrm{opt}}, \boldsymbol{P}_{\mathrm{opt}}, g_{\mathrm{opt}}, \mathcal{O}_{\mathrm{opt}}\} = \underset{\{\boldsymbol{F}, \boldsymbol{P}, g, \mathcal{O}\}}{\mathrm{argmin}} \ \phi \tag{4}$$

$$\text{s.t.} \quad \mathrm{E}\left[\|\boldsymbol{y}[n]\|_2^2 \right] = E_{\mathrm{tr}} \tag{5}$$

$$\boldsymbol{S}_i \boldsymbol{F} \boldsymbol{e}_i = \boldsymbol{0} \quad \text{for} \quad i = 1, \ldots, B$$

[1] Figs. 2 and 3 are fully equivalent. In fact, Fig. 3 still includes the modulo operators represented by the signals $\boldsymbol{\alpha}[n]$ and $\hat{\boldsymbol{\alpha}}[n]$.

where $\boldsymbol{S}_i = [\boldsymbol{I}_i, \boldsymbol{0}_{i\times B-i}] \in \{0,1\}^{i\times B}$ and $\boldsymbol{e}_i$ is the i-th column of the $B \times B$ identity matrix. Using Lagrangian multipliers we obtain the THP filters depending on the precoding order $\mathcal{O}$

$$\begin{aligned}\boldsymbol{F}_{\text{opt}} &= \boldsymbol{I} - \sum_{i=1}^{B} \boldsymbol{\Pi}\boldsymbol{\Phi}^{-1}\boldsymbol{\Pi}^{\mathrm{T}}\boldsymbol{S}_i^{\mathrm{T}}(\boldsymbol{S}_i\boldsymbol{\Pi}\boldsymbol{\Phi}^{-1}\boldsymbol{\Pi}^{\mathrm{T}}\boldsymbol{S}_i^{\mathrm{T}})^{-1}\boldsymbol{S}_i\boldsymbol{e}_i\boldsymbol{e}_i^{\mathrm{T}},\\ \boldsymbol{P}_{\text{opt}} &= g_{\text{opt}}^{-1}\sum_{i=1}^{B} \boldsymbol{H}^{\mathrm{H}}\boldsymbol{\Pi}^{\mathrm{T}}\boldsymbol{S}_i^{\mathrm{T}}(\boldsymbol{S}_i\boldsymbol{\Pi}\boldsymbol{\Phi}^{-1}\boldsymbol{\Pi}^{\mathrm{T}}\boldsymbol{S}_i^{\mathrm{T}})^{-1}\boldsymbol{S}_i\boldsymbol{e}_i\boldsymbol{e}_i^{\mathrm{T}},\end{aligned}$$

where

$$\boldsymbol{\Phi} = (\boldsymbol{H}\boldsymbol{H}^{\mathrm{H}} + \xi\boldsymbol{I})^{-1} \quad \text{and} \quad \xi = \operatorname{tr}(\boldsymbol{\Phi}_{\eta\eta})/E_{\text{tr}}. \tag{6}$$

Since $\boldsymbol{\Phi}$ is Hermitian, its Cholesky factorization with symmetric permutation reads as

$$\boldsymbol{\Pi}\boldsymbol{\Phi}\boldsymbol{\Pi}^{\mathrm{T}} = \boldsymbol{L}^{\mathrm{H}}\boldsymbol{D}\boldsymbol{L}, \tag{7}$$

where $\boldsymbol{L}$ is a *unit lower triangular* matrix and $\boldsymbol{D}$ a *diagonal* matrix. Using (7), the above expressions for the THP filters can be rewritten as

$$\boldsymbol{F}_{\text{opt}} = \boldsymbol{I} - \boldsymbol{L}^{-1}, \qquad \boldsymbol{P}_{\text{opt}} = g_{\text{opt}}^{-1}\boldsymbol{H}^{\mathrm{H}}\boldsymbol{\Pi}^{\mathrm{T}}\boldsymbol{L}^{\mathrm{H}}\boldsymbol{D}. \tag{8}$$

With (8), the MSE from (3) can be expressed as

$$\phi = \operatorname{tr}(\boldsymbol{\Phi}_{\varepsilon\varepsilon}) = \xi\operatorname{tr}(\boldsymbol{\Phi}_{vv}\boldsymbol{D}) = \xi\sum_{i=1}^{B}\sigma_{v_i}^2 d_i. \tag{9}$$

The Cholesky factorization (7) can be calculated iteratively such that the MSE in (9) is minimized. The precoding order $\mathcal{O}$ is determined this way. The Cholesky factorization algorithm is described in detail in [11].

There are two different variants of THP. We can either calculate the weight g_{opt} such that (5) is fullfiled based on the assumed statistics of $\boldsymbol{v}[n]$, or we can calculate g_{opt} such that the power, averaged over a transmit block of length N_{B}, fulfills the power constraint, i.e.,

$$\frac{1}{N_{\text{B}}}\sum_{i=1}^{N_{\text{B}}}\|\boldsymbol{y}[n]\|_2^2 = E_{\text{tr}}. \tag{10}$$

We use the second approach to conform with our general system description from Section II.

IV. Vector Precoding

We now review the MMSE vector precoder as described in [14]. Fig. 4 depicts the system model. The perturbation vector $\boldsymbol{\alpha}[n] \in \tau\mathbb{Z}^B + \mathrm{j}\,\tau\mathbb{Z}^B$ is first added to the signal $\boldsymbol{s}[n]$ and the sum $\boldsymbol{d}[n]$ is then filtered with the linear filter $\boldsymbol{P}$, such that the MSE

$$\phi(\boldsymbol{\alpha}[n], \boldsymbol{y}[n], g) = \frac{1}{N_{\text{B}}}\sum_{n=1}^{N_{\text{B}}}\mathrm{E}\left[\left\|\boldsymbol{d}[n] - \hat{\boldsymbol{d}}[n]\right\|_2^2 \,\middle|\, \boldsymbol{s}[n]\right], \tag{11}$$

averaged over a block of length N_{B}, is minimized. Note that the expectation in the above MSE definition is conditioned on the data signal $\boldsymbol{s}[n]$, since $\boldsymbol{s}[n]$ is known to the transmitter. The optimization problem reads as

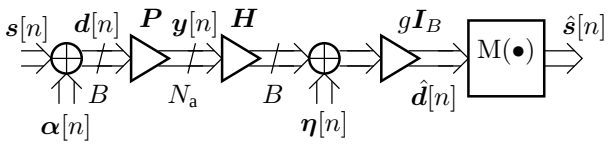

Fig. 4. Vector Precoder System Model.

$$\{\boldsymbol{\alpha}_{\text{opt}}[n], \boldsymbol{y}_{\text{opt}}[n], g_{\text{opt}}\} = \underset{\{\boldsymbol{\alpha},\boldsymbol{y},g\}}{\operatorname{argmin}}\,\phi(\boldsymbol{\alpha}[n], \boldsymbol{y}[n], g) \tag{12}$$

$$\text{s.t.} \qquad \frac{1}{N_{\text{B}}}\sum_{n=1}^{N_{\text{B}}}\|\boldsymbol{y}[n]\|_2^2 = E_{\text{tr}} \tag{13}$$

and using Lagrangian multipliers, the solution is found to be

$$\boldsymbol{y}_{\text{opt}}[n] = g_{\text{opt}}^{-1}\boldsymbol{H}^{\mathrm{H}}(\boldsymbol{H}\boldsymbol{H}^{\mathrm{H}} + \xi\boldsymbol{I}_B)^{-1}\boldsymbol{d}[n], \tag{14}$$

where g_{opt} is chosen such that it fulfills the transmit power constraint (13). With (14), the MSE in (11) becomes

$$\phi(\boldsymbol{\alpha}[n], \boldsymbol{y}[n], g) = \frac{\xi}{N_{\text{B}}}\sum_{n=1}^{N_{\text{B}}}(\boldsymbol{s}[n] + \boldsymbol{\alpha}[n])^{\mathrm{H}}\boldsymbol{\Phi}(\boldsymbol{s}[n] + \boldsymbol{\alpha}[n]).$$

The matrix $\boldsymbol{\Phi}$ and the scalar ξ can be found in (6). Obviously, the n-th summand of $\phi(\boldsymbol{\alpha}[n], \boldsymbol{y}[n], g)$ only depends on $\boldsymbol{\alpha}[n]$. Therefore, each summand of the MSE $\phi(\boldsymbol{\alpha}[n], \boldsymbol{y}[n], g)$ can be minimized separately by choosing the respective perturbation vector:

$$\boldsymbol{\alpha}_{\text{opt}}[n] = \underset{\boldsymbol{\alpha}[n]\in\tau\mathbb{Z}^B+\mathrm{j}\,\tau\mathbb{Z}^B}{\operatorname{argmin}}\left\|\boldsymbol{D}^{1/2}\boldsymbol{L}(\boldsymbol{s}[n] + \boldsymbol{\alpha}[n])\right\|_2^2, \tag{15}$$

where we used the Cholesky factorization $\boldsymbol{\Phi} = \boldsymbol{L}^{\mathrm{H}}\boldsymbol{D}\boldsymbol{L}$. The matrices $\boldsymbol{D}$ and $\boldsymbol{L}$ have the same properties as in (7). We used the specific Cholesky factorization so as to conform with the THP reference model from Section III.[2] Note that the calculation of $\boldsymbol{\alpha}[n]$ in (15) results from a closest point search in a B-dimensional lattice [18], which makes VP computationally intensive.

V. Scaled Vector Precoding

A. System Model

In our novel system, we combine the architectures of THP and VP (see also [9]). The system model is depicted in Fig. 5. Although the loopback is obsolete, it is necessary for the derivation of the optimum precoding order. The permuted perturbation vector $\boldsymbol{\alpha}'[n] = \boldsymbol{\Pi}\boldsymbol{\alpha}[n]$ is split into B/p groups of p consecutive elements:[3]

$$\begin{aligned}\boldsymbol{\alpha}'[n] &= \left[\boldsymbol{\alpha}_1'[n], \ldots, \boldsymbol{\alpha}_{B/p}'[n]\right]^{\mathrm{T}},\\ \boldsymbol{\alpha}_i'[n] &= [\alpha_{pi-p+1}'[n], \ldots, \alpha_{pi}'[n]]^{\mathrm{T}}, \quad i = 1, \ldots, B/p.\end{aligned} \tag{16}$$

The p elements of every group are computed jointly, but contrary to VP, the elements of the other groups are assumed to be constant. Note that we do not make any specific assumptions for the computation of the perturbation signal $\boldsymbol{\alpha}[n]$ besides the

[2] We could in fact use any square root of $\boldsymbol{\Phi}$

[3] For notational simplicity, we assume that B is an integer multiple of p.

constraint that the entries are computed p-elements-wise. This is in contrast to THP, where the element-wise computation of $\boldsymbol{\alpha}[n]$ results from the modulo operator $\mathrm{M}(\bullet)$. The groups of p elements of $\boldsymbol{\Pi}\boldsymbol{d}[n]$, corresponding to $\boldsymbol{\alpha}'_1[n], \ldots, \boldsymbol{\alpha}'_{B/p}[n]$, are then circulated in the loop in B/p iterations. This scheme is thus operating with vectors of length p instead of single elements like THP. Note that p is a system parameter and does not take part in the optimization. The feedback matrix $\boldsymbol{F}$ has again a lower triangular structure but its $p \times p$ diagonal blocks are zero, since the p elements of one group $\boldsymbol{\alpha}'_i[n]$ are computed jointly and can only be fed back after computation. At this point, we assume that the elements of $\boldsymbol{v}[n]$ are correlated only inside the p-groups and thus, $\boldsymbol{\Phi}_{vv}$ has a block diagonal structure with $p \times p$ blocks on the diagonal. When $p = 1$, our system converges to THP with the exception that in our case, $\boldsymbol{\alpha}[n]$ is not constrained to evolve from the modulo operation $\mathrm{M}(\bullet)$. However, these two schemes are equivalent, as we will see later. When $p = B$, we calculate all elements of $\boldsymbol{\alpha}[n]$ jointly in one step and our system converges to VP from Section IV.

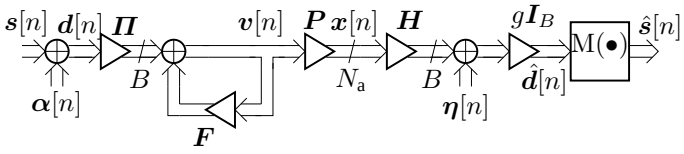

Fig. 5. Scaled Vector Precoding Reference Model.

B. MMSE Scaled Vector Precoding

In the MMSE approach, we try to minimize the MSE of $\hat{\boldsymbol{d}}[n]$ with respect to $\boldsymbol{d}[n]$, i.e., the variance of the error signal $\boldsymbol{\varepsilon}[n] = \boldsymbol{d}[n] - \hat{\boldsymbol{d}}[n]$. From Fig. 5, we have that

$$\hat{\boldsymbol{d}}[n] = g\boldsymbol{H}\boldsymbol{P}\boldsymbol{v}[n] + g\boldsymbol{\eta}[n]. \tag{17}$$

The output signal of the feedback loop with the feedback filter $\boldsymbol{F}$ is $\boldsymbol{v}[n] = \boldsymbol{\Pi}\boldsymbol{d}[n] + \boldsymbol{F}\boldsymbol{v}[n]$, which yields

$$\boldsymbol{d}[n] = \boldsymbol{\Pi}^{\mathrm{T}}(\boldsymbol{I} - \boldsymbol{F})\boldsymbol{v}[n].$$

Thus, the MSE is given by

$$\begin{aligned}\phi \;&=\; \mathrm{E}\left[\|\boldsymbol{\varepsilon}\|_2^2\right] = \mathrm{tr}(\boldsymbol{\Phi}_{\varepsilon\varepsilon}) = \\ &= \mathrm{tr}\left((\boldsymbol{I} - \boldsymbol{F})\boldsymbol{\Phi}_{vv}(\boldsymbol{I} - \boldsymbol{F}^{\mathrm{H}}) + g^2\boldsymbol{H}\boldsymbol{P}\boldsymbol{\Phi}_{vv}\boldsymbol{P}^{\mathrm{H}}\boldsymbol{H}^{\mathrm{H}}\right. \\ &\quad -g\boldsymbol{\Pi}^{\mathrm{T}}(\boldsymbol{I} - \boldsymbol{F})\boldsymbol{\Phi}_{vv}\boldsymbol{P}^{\mathrm{H}}\boldsymbol{H}^{\mathrm{H}} - g\boldsymbol{H}\boldsymbol{P}\boldsymbol{\Phi}_{vv}(\boldsymbol{I} - \boldsymbol{F}^{\mathrm{H}})\boldsymbol{\Pi} \\ &\quad \left.+g^2\boldsymbol{\Phi}_{\eta\eta}\right). \end{aligned} \tag{18}$$

The optimization problem for MMSE-SVP reads as

$$\{\boldsymbol{F}_{\text{opt}}, \boldsymbol{P}_{\text{opt}}, g_{\text{opt}}, \mathcal{O}_{\text{opt}}, \boldsymbol{\alpha}_{\text{opt}}[n]\} = \underset{\{\boldsymbol{F},\boldsymbol{P},g,\mathcal{O},\boldsymbol{\alpha}[n]\}}{\operatorname{argmin}} \quad \phi \tag{19}$$

$$\text{s.t.} \qquad \frac{1}{N_\mathrm{B}} \sum_{i=1}^{N_\mathrm{B}} \|\boldsymbol{y}[n]\|_2^2 = E_{\text{tr}} \tag{20}$$

$$\boldsymbol{S}_{pi}\boldsymbol{F}(\boldsymbol{e}_i \otimes \boldsymbol{I}_p) = \boldsymbol{0} \quad \text{for} \quad i = 1, \ldots, B/p \tag{21}$$

where $\boldsymbol{e}_i$ is now the i-th vector of the $(B/p \times B/p)$ identity matrix and $\boldsymbol{S}_i = [\boldsymbol{I}_i, \boldsymbol{0}_{i\times B-i}] \in \{0,1\}^{i\times B}$. The last constraint (21) ensures that the feedback filter $\boldsymbol{F}$ is lower triangular with $p\times p$ zero blocks on the main diagonal. This structural property of the feedback filter $\boldsymbol{F}$ is necessary, since the perturbation vector is computed group-wise. The precoding order $\mathcal{O}_{\text{opt}}$ will be found later through a modified Cholesky factorization algorithm and the rule to find the perturbation signal $\boldsymbol{\alpha}_{\text{opt}}[n]$ will be obtained in a final step. Using Lagrangian multipliers, we obtain

$$\boldsymbol{F}_{\text{opt}} = \boldsymbol{I} - \sum_{i=1}^{B/p} \boldsymbol{\Pi}\boldsymbol{\Phi}^{-1}\boldsymbol{\Pi}^{\mathrm{T}}\boldsymbol{S}_{pi}^{\mathrm{T}}(\boldsymbol{S}_{pi}\boldsymbol{\Pi}\boldsymbol{\Phi}^{-1}\boldsymbol{\Pi}^{\mathrm{T}}\boldsymbol{S}_{pi}^{\mathrm{T}})^{-1}\boldsymbol{S}_{pi}(\boldsymbol{e}_i\boldsymbol{e}_i^{\mathrm{T}} \otimes \boldsymbol{I}_p)$$

$$\boldsymbol{P}_{\text{opt}} = g^{-1}\sum_{i=1}^{B/p} \boldsymbol{H}^{\mathrm{H}}\boldsymbol{\Pi}^{\mathrm{T}}\boldsymbol{S}_{pi}^{\mathrm{T}}(\boldsymbol{S}_{pi}\boldsymbol{\Pi}\boldsymbol{\Phi}^{-1}\boldsymbol{\Pi}^{\mathrm{T}}\boldsymbol{S}_{pi}^{\mathrm{T}})^{-1}\boldsymbol{S}_{pi}(\boldsymbol{e}_i\boldsymbol{e}_i^{\mathrm{T}} \otimes \boldsymbol{I}_p).$$

Note that $\boldsymbol{F}_{\text{opt}}$ and $\boldsymbol{P}_{\text{opt}}$ depend on the precoding order $\mathcal{O}$, since the permutation matrix $\boldsymbol{\Pi}$ is a function of $\mathcal{O}$ (see Eq. 2). At this point, we perform a modified *block* Cholesky factorization of $\boldsymbol{\Phi}$ with symmetric permutation

$$\boldsymbol{\Pi}\boldsymbol{\Phi}\boldsymbol{\Pi}^{\mathrm{T}} = \boldsymbol{L}^{\mathrm{H}}\boldsymbol{D}\boldsymbol{L}, \tag{22}$$

where $\boldsymbol{L}$ is a *block unit lower triangular* matrix with $p \times p$ identity submatrices on the main diagonal, and $\boldsymbol{D}$ is a positive definite *block diagonal* matrix with $p \times p$ submatrices on the main diagonal. Employing (22), we get for the MMSE-SVP filters:

$$\boldsymbol{F}_{\text{opt}} = \boldsymbol{I} - \boldsymbol{L}^{-1}, \qquad \boldsymbol{P}_{\text{opt}} = g_{\text{opt}}^{-1}\boldsymbol{H}^{\mathrm{H}}\boldsymbol{\Pi}^{\mathrm{T}}\boldsymbol{L}^{\mathrm{H}}\boldsymbol{D}. \tag{23}$$

This result is analogous to (8). Nevertheless, the matrices $\boldsymbol{L}$ and $\boldsymbol{D}$ now have a $p\times p$-block structure, in contrast to (7). We can calculate g_{opt} using the transmit power constraint in (20). Using (23) and (18) together with g_{opt} resulting from (23), the MSE becomes

$$\phi = \mathrm{tr}(\boldsymbol{\Phi}_{\varepsilon\varepsilon}) = \xi\,\mathrm{tr}(\boldsymbol{\Phi}_{vv}\boldsymbol{D}). \tag{24}$$

Now we make the assumption that the elements of $\boldsymbol{v}[n]$ are in fact uncorrelated. This assumption is supported by simulation results which show that the correlation inside the groups of p elements is weak. Thus, $\boldsymbol{\Phi}_{vv} = \mathrm{diag}(\sigma_{v_1}^2, \ldots, \sigma_{v_B}^2)$, where the variances $\sigma_{v_i}^2$ inside a group of p elements is the same, i.e., $\sigma_{v_i}^2 = \sigma_{\text{group},j}^2, \forall i \in \{(j-1)p+1, \ldots, jp\}$. Under this simplifying assumption,[4] the MSE in (24) can be written as

$$\phi = \xi\sum_{i=1}^{B}\sigma_{v_i}^2 d_i. \tag{25}$$

The resulting MSE depends on the variances $\sigma_{v_i}^2$ and the diagonal entries of $\boldsymbol{D}$. We see that the optimality of the filter solution (23) depends on the calculation of the block Cholesky factorization (22) via the diagonal entries of $\boldsymbol{D}$ in the MSE. Since the block Cholesky factorization (22) is a function of the permutation matrix $\boldsymbol{\Pi}$, (24) tells us how to choose the precoding order $\mathcal{O}$: We have to compute (22) such that $\sum_{i=1}^{B}\sigma_{v_i}^2 d_i$ is minimized. The minimization of the

[4]For the algorithm in Table I, this assumption was made. The algorithm can be rewritten to take account of the correlations inside a group. However, the covariance matrix $\boldsymbol{\Phi}_{vv}$ has to be known in this case, that is, it must be estimated.

TABLE I

CALCULATION OF THE BLOCK CHOLESKY FACTORIZATION

factorize: $\boldsymbol{\Pi\Phi\Pi}^{\mathrm{T}} = \boldsymbol{L}^{\mathrm{H}}\boldsymbol{DL}$ (find: $\boldsymbol{\Pi}, \boldsymbol{L}, \boldsymbol{D}$)
$\boldsymbol{\Pi} = \boldsymbol{I}_B,\ \boldsymbol{D} = \boldsymbol{0}_B$
for $i = B/p, \ldots, 1$
  $\boldsymbol{k} = [pi - p + 1, pi - p + 2, \ldots, pi]$
  $\boldsymbol{m} = [1, 2, \ldots, pi - p]$
  find the p smallest values of $\mathrm{diag}(\boldsymbol{\Phi}(1 : pi, 1 : pi))$ and place their indices in $\boldsymbol{q}$
  $\boldsymbol{\Pi}_i = \boldsymbol{I}_B$ whose rows $\boldsymbol{k}$ are exchanged with the rows with indices $\boldsymbol{q}$
  $\boldsymbol{\Pi} = \boldsymbol{\Pi}_i\boldsymbol{\Pi}$
  $\boldsymbol{\Phi} = \boldsymbol{\Pi}_i\boldsymbol{\Phi}\boldsymbol{\Pi}_i$
  $\boldsymbol{D}(\boldsymbol{k}, \boldsymbol{k}) = \boldsymbol{\Phi}(\boldsymbol{k}, \boldsymbol{k})$
  $\boldsymbol{\Phi}(1 : pi, \boldsymbol{k}) = \boldsymbol{\Phi}(1 : pi, \boldsymbol{k})\boldsymbol{D}^{-1}(\boldsymbol{k}, \boldsymbol{k})$
  $\boldsymbol{\Phi}(\boldsymbol{m}, \boldsymbol{m}) = \boldsymbol{\Phi}(\boldsymbol{m}, \boldsymbol{m}) - \boldsymbol{\Phi}(\boldsymbol{m}, \boldsymbol{k} : pi)\boldsymbol{D}(\boldsymbol{k}, \boldsymbol{k})\boldsymbol{\Phi}^{\mathrm{H}}(\boldsymbol{m}, \boldsymbol{k} : pi)$
$\boldsymbol{L}^{\mathrm{H}}$ = upper triangular part of $\boldsymbol{\Phi}$

whole sum is a difficult combinatorial problem, because all possible combinations of data streams in groups have to be tested. Therefore, we propose a suboptimal algorithm which computes the factorization successively trying to minimize every summand of the MSE in (25) separately under the assumption that the indices of the groups to be precoded later are already fixed. Note that the values of $\sigma_{v_i}^2$ are not necessary for this heuristic rule, since we assumed that $\sigma_{v_i}^2$ is equal inside a group of p elements. Table I summarizes the pseudo code of the proposed block Cholesky factorization. The factorization algorithm in [11] is a special case of the proposed algorithm in Table I, for $p = 1$.

We conclude with the computation of the perturbation vector $\boldsymbol{\alpha}[n] = \boldsymbol{\Pi}^{\mathrm{T}}\boldsymbol{\alpha}'[n]$. As mentioned earlier, the perturbation vector $\boldsymbol{\alpha}[n]$ is computed group-wise, i.e., the p entries of $\boldsymbol{\alpha}[n]$ corresponding to the i-th group are found for fixed values of the groups $1, \ldots, i-1$.

When replacing the covariance matrix $\boldsymbol{\Phi}_{vv}$ by its sample mean estimate $\sum_{n=1}^{N_{\mathrm{B}}} \boldsymbol{v}[n]\boldsymbol{v}^{\mathrm{H}}[n]/N_{\mathrm{B}}$ in the MSE expression (24), we get

$$\phi = \frac{\xi}{N_{\mathrm{B}}} \sum_{n=1}^{N_{\mathrm{B}}} \left(\boldsymbol{\Pi}\boldsymbol{s}[n] + \boldsymbol{\alpha}'[n]\right)^{\mathrm{H}} \boldsymbol{L}^{\mathrm{H}}\boldsymbol{DL} \left(\boldsymbol{\Pi}\boldsymbol{s}[n] + \boldsymbol{\alpha}'[n]\right). \tag{26}$$

Here, we used $\boldsymbol{v}[n] = \boldsymbol{\Pi}(\boldsymbol{s}[n] + \boldsymbol{\alpha}[n]) + \boldsymbol{F}\boldsymbol{v}[n]$ and (23). We observe that the n-th summand only depends on the n-th perturbation vector and is independent of the other $N_{\mathrm{B}} - 1$ perturbation vectors. Thus, the perturbation vectors can be found separately by minimizing the respective summand. Obviously, minimizing the n-th summand of the above MSE is equivalent to the VP rule in (15), if no restrictions are imposed on the computation of $\boldsymbol{\alpha}[n]$.

We define the projector matrix

$$\boldsymbol{\Pi}_i = \sum_{j=1}^{i} \boldsymbol{e}_i\boldsymbol{e}_i^{\mathrm{T}} \tag{27}$$

which leaves the first i entries of a column vector unchanged and sets the other elements to zero, when applied from the left. The projection with $\boldsymbol{\Pi}_i$ is used to include the restriction in the rule for the computation of the perturbation vector that the elements of the j-th group are computed based only on the already computed elements of the previous $j - 1$ groups. The proposed heuristic rule reads as

$$\boldsymbol{\alpha}'_{i,\mathrm{opt}}[n] = \underset{\boldsymbol{\alpha}'_i[n] \in \tau\mathbb{Z}^p + \mathrm{j}\,\tau\mathbb{Z}^p}{\operatorname{argmin}} \left\| \boldsymbol{D}^{1/2}\boldsymbol{\Pi}_{pi}\boldsymbol{L}\boldsymbol{\Pi}_{pi}(\boldsymbol{\Pi}\boldsymbol{s}[n] + \boldsymbol{\alpha}'[n]) \right\|_2^2 \quad \text{for } i = 1, \ldots, B/p \tag{28}$$

where $\boldsymbol{\alpha}'_i[n]$ is given in (16). Due to the right projector matrix $\boldsymbol{\Pi}_{pi}$, only the parts $[s_{k_1}, \ldots, s_{k_{pi}}, 0, \ldots, 0]^{\mathrm{T}}$ and $[\boldsymbol{\alpha}'^{,\mathrm{T}}_{1,\mathrm{opt}}, \ldots, \boldsymbol{\alpha}'^{,\mathrm{T}}_{i-1,\mathrm{opt}}, \boldsymbol{\alpha}'^{,\mathrm{T}}_{i}, 0, \ldots, 0]^{\mathrm{T}}$ of the vectors $\boldsymbol{s}[n]$ and $\boldsymbol{\alpha}'[n]$, respectively, are used. Hence, the value of $\boldsymbol{\alpha}'_{i,\mathrm{opt}}[n]$ depends only on the previously calculated parts $\boldsymbol{\alpha}'_{j,\mathrm{opt}}[n]$ for $j = 1, \ldots, i-1$.

When $p = 1$, the block Cholesky factorization in (22) is the same as the Cholesky factorization in (7). Consequently, the filters in (23) are equal to the filters in (8). As shown in Appendix I, the perturbation vector $\boldsymbol{\alpha}[n]$ computed by (28) is the same with the perturbation vector calculated by the modulo operator in the loop of the THP. Thus, for $p = 1$ this scheme merges to the THP of Section III.

When $p = B$, $\boldsymbol{\Pi}_{pi} = \boldsymbol{I}_B$ and the decision rule is the same as (15). Furthermore, the block Cholesky factorization breaks down to $\boldsymbol{\Pi\Phi\Pi}^{\mathrm{T}} = \boldsymbol{D}$ and $\boldsymbol{L} = \boldsymbol{I}$. The filters (23) become

$$\boldsymbol{F}_{\mathrm{opt},p=B} = \boldsymbol{0}, \qquad \boldsymbol{P}_{\mathrm{opt},p=B} = g_{\mathrm{opt}}^{-1}\boldsymbol{H}^{\mathrm{H}}\boldsymbol{\Phi}\boldsymbol{\Pi}^{\mathrm{T}} \tag{29}$$

and the transmit vector $\boldsymbol{y}[n]$ is

$$\boldsymbol{y}[n] = \boldsymbol{P}\boldsymbol{\Pi}(\boldsymbol{s}[n] + \boldsymbol{\alpha}_{\mathrm{opt}}[n]) = g_{\mathrm{opt}}^{-1}\boldsymbol{H}^{\mathrm{H}}\boldsymbol{\Phi}\boldsymbol{d}[n], \tag{30}$$

which is the same as (14). So, for $p = B$ this scheme merges to VP of Section IV.

For values of p between 1 and B we get a hybrid system whose performance lies between THP and VP. The complexity of this scheme is dominated by the lattice search in (28). The search for the optimum vector is performed in a p-dimensional (complex) lattice. Consequently, the complexity also lies between those of THP and VP. For the case where $p = 1$, the search is actually a simple quantization operation and the complexity is the same as that of THP.

C. Equivalent System

As we saw, the loopback of Fig. 5 is obsolete. This allows us to use an equivalent model with only one linear filter—the concatenation of $\boldsymbol{F}$, $\boldsymbol{P}$ and $\boldsymbol{\Pi}$. The equivalent model is the same as in Fig. 4, with the linear filter

$$\boldsymbol{P}_{\mathrm{eq.}} = \boldsymbol{P}(\boldsymbol{I} - \boldsymbol{F})^{-1}\boldsymbol{\Pi} = g_{\mathrm{opt}}^{-1}\boldsymbol{H}^{\mathrm{H}}\boldsymbol{\Phi}. \tag{31}$$

The linear filter is simply a zero-forcing or MMSE filter (according to the design criterion). The perturbation vector $\boldsymbol{\alpha}[n]$ is computed beforehand following the rule (28). It is now clear that the final scheme can be seen as *scaled vector precoding* (SVP). The parameter p scales the operation and switches from VP ($p = B$), through some intermediate modes, until THP ($p = 1$). The model depicted in Fig. 5 was necessary for finding the rule in (28) and for showing the equivalence with THP.

D. Using the Real-Valued Model

We can as well apply the above analysis to the real-valued representation of a MIMO system. The resulting dimensionality is twice the dimensionality of the complex-valued model. Thus, the operation mode p takes one more value, from $p = 1$ up to $p = 2B$. As shown in [19], using the real-valued representation for successive interference cancellation (here, the case $p = 1$–THP) yields a better performance than using the complex-valued representation. This gain results from the separation of the real and imaginary part of a data stream, which are not forced to be precoded together in the real-valued representation. However, recall that the real-valued channel matrix is given by

$$\boldsymbol{H}_{\mathrm{r}} = \begin{bmatrix} \Re\{\boldsymbol{H}\} & -\Im\{\boldsymbol{H}\} \\ \Im\{\boldsymbol{H}\} & \Re\{\boldsymbol{H}\} \end{bmatrix}. \tag{32}$$

From (32) we see that the diagonal values of $\boldsymbol{H}_{\mathrm{r}}$ come always in pairs which correspond to one data stream. This is also true for $\boldsymbol{\Phi} = (\boldsymbol{H}\boldsymbol{H}^{\mathrm{H}} + \xi\boldsymbol{I})^{-1}$. Since the factorization algorithm of Table I sorts the diagonal values of $\boldsymbol{\Phi}$, the streams corresponding to the same data stream will be selected at the same time, when $p = 2, \ldots, 2B$. But since the real and imaginary part of each data stream are not separated, we obtain the same precoding order as in the complex-valued representation. Hence, the performance for some value of p in the complex-valued representation is the same as for $2p$ in the real-valued representation. Using the real-valued representation is only meaningful for $p = 1$ (regular THP).

VI. Lattice-Reduction Aided Scaled Vector Precoding

Lattice-reduction techniques have become very popular due to their superior performance [20]. In fact, lattice-reduction aided detection and precoding yield the full channel diversity at low complexity. The most popular algorithm used for lattice-reduction is the Lenstra, Lenstra, Lovász (LLL) algorithm, which has polynomial complexity [21]. Windpassinger substituted the closest-point search in VP (see Eq. 15) with Babai's approximate solutions (see [17]), namely the *rounding-off* and the *nearest-plane* approximation [13]. These algorithms operate in an LLL-reduced basis instead of the initial one. The rounding-off procedure is similar to linear equalization and the nearest-plane algorithm is similar to decision-feedback equalization (DFE). The approximate solution of the nearest-plane algorithm for $\boldsymbol{\alpha}[n]$ is computed through successice elementwise quantization, taking into account previously quantized values. The performance can be further improved by choosing the appropriate precoding order. The complexity of this scheme is the same as the complexity of DFE (or THP) and the resulting BER curve is remarkably close to VP, as shown in [13]. Our heuristic rule (28) avoids the closest-point search of VP by computing the values of $\boldsymbol{\alpha}[n]$ elementwise ($p = 1$). As a matter of fact, the case $p = 1$ of SVP corresponds to Babai's nearest-plane approximation with optimized order, with the difference that the lattice basis has not been reduced.

In the following, we will combine lattice-reduction with the proposed SVP. Since the LLL algorithm operates on real matrices, we use the real-valued representation for the MIMO system. This will be indicated in the following with the index 'r'. We start with (26) and write the closest-point search as

$$\boldsymbol{\alpha}_{\mathrm{opt,r}}[n] = \underset{\boldsymbol{\alpha}_{\mathrm{r}}[n]\in\tau\mathbb{Z}^{2B}}{\operatorname{argmin}} (\boldsymbol{s}_{\mathrm{r}}[n]+\boldsymbol{\alpha}_{\mathrm{r}}[n])^{\mathrm{H}}\boldsymbol{\Phi}_{\mathrm{r}}(\boldsymbol{s}_{\mathrm{r}}[n]+\boldsymbol{\alpha}_{\mathrm{r}}[n]), \tag{33}$$

where $\boldsymbol{\alpha}_{\mathrm{r}}[n] = [\Re(\boldsymbol{\alpha}^{\mathrm{T}}[n]), \Im(\boldsymbol{\alpha}^{\mathrm{T}}[n]]^{\mathrm{T}}$ and $\boldsymbol{\Phi}_{\mathrm{r}}$ depends on $\boldsymbol{\Phi}$ as $\boldsymbol{H}_{\mathrm{r}}$ on $\boldsymbol{H}$ in (32). First, we perform the Cholesky factorization $\boldsymbol{\Phi}_{\mathrm{r}} = \boldsymbol{\Gamma}^{\mathrm{H}}\boldsymbol{\Gamma}$ and then we apply the LLL algorithm on $\boldsymbol{\Gamma}$ and obtain $\boldsymbol{\Gamma}_{\mathrm{red}} = \boldsymbol{\Gamma}\boldsymbol{T}$ with the reduced basis $\boldsymbol{\Gamma}_{\mathrm{red}}$ and $\boldsymbol{T}$ is the unimodular transformation matrix [22]. The rule (33) can be rewritten as

$$\begin{aligned}
\boldsymbol{\alpha}_{\mathrm{opt,r}}[n] &= \tau \underset{\boldsymbol{z}_{\mathrm{r}}[n]\in\mathbb{Z}^{2B}}{\operatorname{argmin}} \|\boldsymbol{\Gamma}(\boldsymbol{s}_{\mathrm{r}}[n] + \tau\boldsymbol{z}_{\mathrm{r}}[n])\|_2^2 \\
&= \tau \underset{\boldsymbol{z}_{\mathrm{r}}[n]\in\mathbb{Z}^{2B}}{\operatorname{argmin}} \left\| \frac{1}{\tau}\boldsymbol{\Gamma}\boldsymbol{s}_{\mathrm{r}}[n] + \boldsymbol{\Gamma}_{\mathrm{red}}\boldsymbol{T}^{-1}\boldsymbol{z}_{\mathrm{r}}[n] \right\|_2^2 \\
&= \tau\boldsymbol{T} \underset{\boldsymbol{z}'_{\mathrm{r}}[n]\in\mathbb{Z}^{2B}}{\operatorname{argmin}} \left\| \frac{1}{\tau}\boldsymbol{\Gamma}\boldsymbol{s}_{\mathrm{r}}[n] + \boldsymbol{\Gamma}_{\mathrm{red}}\boldsymbol{z}'_{\mathrm{r}}[n] \right\|_2^2 \\
&= \tau\boldsymbol{T} \underset{\boldsymbol{z}'_{\mathrm{r}}[n]\in\mathbb{Z}^{2B}}{\operatorname{argmin}} (\boldsymbol{s}'_{\mathrm{r}} + \boldsymbol{z}'_{\mathrm{r}})^{\mathrm{H}}\boldsymbol{\Phi}'(\boldsymbol{s}'_{\mathrm{r}} + \boldsymbol{z}'_{\mathrm{r}}),
\end{aligned} \tag{34}$$

where $\boldsymbol{\Phi}' = \boldsymbol{\Gamma}_{\mathrm{red}}^{\mathrm{H}}\boldsymbol{\Gamma}_{\mathrm{red}}$ and $\boldsymbol{s}'_{\mathrm{r}} = \frac{1}{\tau}\boldsymbol{T}^{-1}\boldsymbol{s}_{\mathrm{r}}$. We used the auxiliary variables $\boldsymbol{z}_{\mathrm{r}} = \frac{1}{\tau}\boldsymbol{s}_{\mathrm{r}}$ and $\boldsymbol{z}'_{\mathrm{r}} = \boldsymbol{T}^{-1}\boldsymbol{z}_{\mathrm{r}}$. In (34), we have another expression for the closest-point search of (33). The search is now conducted in an LLL-reduced basis. Following the heuristic utilized for (28) to get a group-wise computation of the perturbation vector, the closest-point search in (28) can be reformulated as

$$\begin{aligned}
\boldsymbol{z}'_{i,\mathrm{r,app,p}}[n] = \underset{\boldsymbol{z}'_{i,\mathrm{r,p}}\in\mathbb{Z}^p}{\operatorname{argmin}} \left\| \boldsymbol{D}^{1/2}\boldsymbol{\Pi}_{pi}\boldsymbol{L}\boldsymbol{\Pi}_{pi}(\boldsymbol{\Pi}\boldsymbol{s}'_{\mathrm{r}}[n] + \boldsymbol{z}'_{\mathrm{r,p}}[n]) \right\|_2^2 \\
\text{for } i = 1, \ldots, 2B/p,
\end{aligned} \tag{35}$$

where the symmetrically permuted block Cholesky factorization is performed on $\boldsymbol{\Phi}'$

$$\boldsymbol{\Pi}\boldsymbol{\Phi}'\boldsymbol{\Pi}^{\mathrm{T}} = \boldsymbol{L}^{\mathrm{H}}\boldsymbol{D}\boldsymbol{L}. \tag{36}$$

The final approximate solution is

$$\boldsymbol{\alpha}_{\mathrm{r,app}}[n] = \tau\boldsymbol{T}\boldsymbol{\Pi}^{\mathrm{T}}\boldsymbol{z}'_{\mathrm{r,app}}. \tag{37}$$

Since the iterative computation in (35) has multiple operation modes, for different values of p, it can be seen as a generalization of Babai's nearest-plane approximation with optimized order.

VII. Simulation Results

The channel used for our simulations has i.i.d. unit variance Rayleigh fading coefficients and emulates an idealized rich-scattering environment. The derivations in Sections III, IV, and V refer to the MMSE approaches. We also simulated the zero-forcing approaches which are directly inherited from the above results, by substituting $\boldsymbol{\Phi}$ in (6) with $\boldsymbol{\Phi} = (\boldsymbol{H}\boldsymbol{H}^{\mathrm{H}})^{-1}$.

Figs. 6 to 9 show the uncoded *bit error rate* (BER) over $E_{\mathrm{b}}/N_0 = \frac{E_{\mathrm{tr}}}{BR_{\mathrm{b}}\sigma_\eta^2}$, where R_{b} is the number of information bits

per channel use and the noise is assumed to be white, that is, $\boldsymbol{\Phi}_{\eta\eta} = \sigma_\eta^2 \boldsymbol{I}$. The modulation alphabet is QPSK ($R_\mathrm{b} = 2$). The lattice search (28) is implemented with the sphere decoder using the Schnorr-Euchner Strategy [18].

Fig. 6 depicts the complex-valued zero-forcing SVP for a 4×4 MIMO-system. We see how the intermediate variant for $p = 2$ lies between the curves of THP and VP, and how optimizing the precoding order improves performance. Fig. 7 compares complex-valued zero-forcing SVP with the real-valued counterpart. We see how for increasing values of p we get higher diversity, since the search for the perturbation vector is performed in higher dimensional lattices. We also verify the observation of Sec. V-D that the performance for some p for the complex-valued model is the same as $2p$ of the real-valued model.

Fig. 8 compares zero-forcing SVP with zero-forcing lattice-reduction SVP (LR-SVP) for a 8×8 MIMO-system. LR-SVP clearly outperforms all variants of SVP for $p < B$. However, the gain of LR-SVP for $p > 1$ is moderate. We can conclude that the most favorable zero-forcing precoding technique is LR-SVP for $p = 1$ (or nearest-plane VP), which has the most attractive balance between low complexity and performance.

Fig. 9 makes the same comparison between the MMSE variants of SVP and LR-SVP. However, in this case the gap between SVP for $p = 1$ (MMSE-THP) and SVP for $p = B$ (MMSE-VP) is very small. Although the intermediate variants of SVP and LR-SVP fill this gap, the gain is moderate compared to the increased complexity. Even LR-SVP for $p = 1$ (nearest-plane VP) is not worth the additional computation of the reduced lattice-basis, since it performs almost like SVP for $p = 1$. Thus, the most favorable MMSE precoding technique is SVP for $p = 1$ (MMSE-THP).

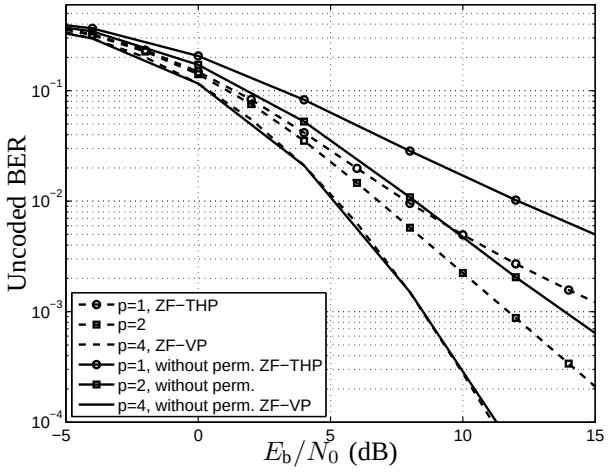

Fig. 6. $B = N_\mathrm{a} = 4$, Zero-Forcing Variant, SVP, with and without Optimized Precoding Order

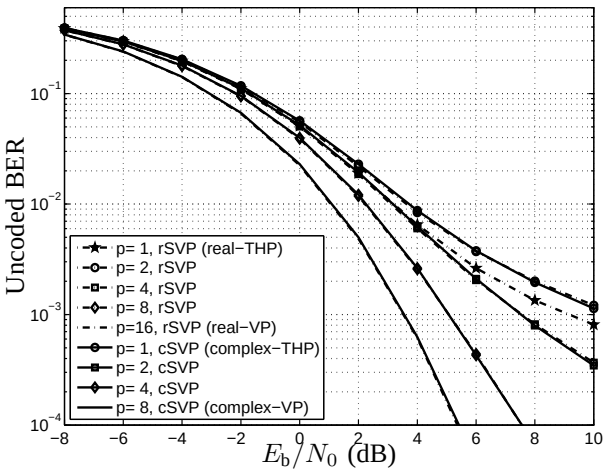

Fig. 7. $B = N_\mathrm{a} = 8$, Zero-Forcing Variant, Complex-Valued SVP (cSVP) vs. Real-Valued SVP (rSVP)

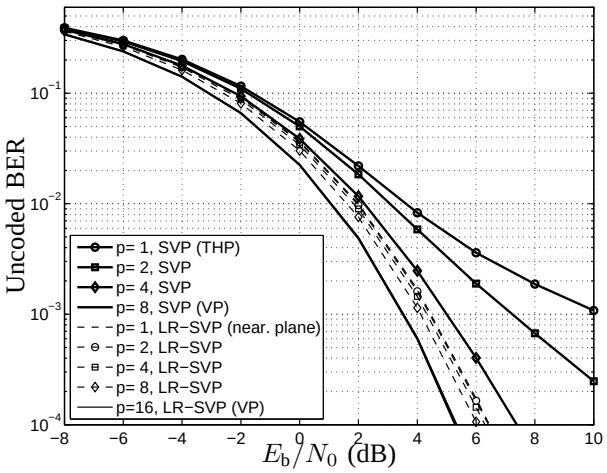

Fig. 8. $B = N_\mathrm{a} = 8$, Zero-Forcing Variant, SVP and LR-SVP

APPENDIX I

When $p = 1$, the decision rule for α_j from (28) takes the form

$$\alpha'_j = -\,\mathrm{Q}\left(s_{k_j} + \sum_{i=1}^{j-1} l_{j,i}\,(s_{k_i} + \hat{\alpha}'_i)\right) \tag{38}$$

where $[\boldsymbol{L}]_{i,j} = l_{i,j}$ and $\mathrm{Q}(\bullet)$ quantizes its argument to the points $\tau\mathbb{Z} + \mathrm{j}\,\tau\mathbb{Z}$. The values $\hat{\alpha}_i,\ i = 1, \ldots, j-1$ have been already computed. s_{k_j} is the j-the element of $\boldsymbol{\Pi s}$.

Meanwhile, the value of $\alpha_{j,\mathrm{THP}}$ in THP can be found from the loop of Fig. 2 as follows

$$\alpha_{j,\mathrm{THP}} = v_j - \tilde{s}_j = \mathrm{M}(\tilde{s}_j) - \tilde{s}_j = -\,\mathrm{Q}(\tilde{s}_j). \tag{39}$$

We will show that the arguments in (38) and (39) are equal. $\tilde{\boldsymbol{s}}$ is calculated after the loopback and in general

$$\tilde{s}_j = s_{k_j} - \sum_{i=1}^{j-1} l_{j,i}^{-1} v_i \tag{40}$$

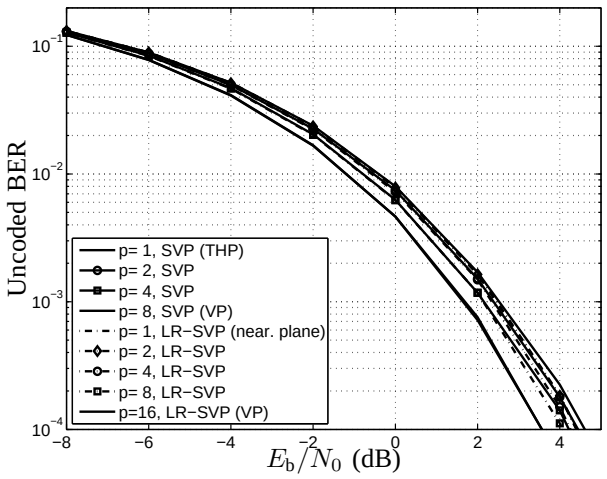

Fig. 9. $B = N_a = 8$, MMSE Variant, SVP and LR-SVP

where $[\boldsymbol{L}^{-1}]_{i,j} = l_{i,j}^{-1}$. Since $\boldsymbol{L}$ is a unit lower triangular matrix, $\boldsymbol{L}^{-1}$ is also unit lower triangular and the elements of $\boldsymbol{L}$ can be easily found as a function of the elements of $\boldsymbol{L}^{-1}$. In fact, by multiplying the j-th row of $\boldsymbol{L}^{-1}$ with the i-th row of $\boldsymbol{L}$ we find the recursive equation

$$l_{j,i} = -\sum_{m=i}^{j-1} l_{j,m}^{-1} l_{m,i} \qquad \text{for } i < j. \tag{41}$$

First, since $l_{1,1} = l_{1,1}^{-1} = 1$ we have that $\alpha_1' = \alpha_{1,\text{THP}} = 0$. Next, since $l_{2,1}^{-1} = -l_{2,1}$ and $\boldsymbol{v}_1 = s_{k_1}$ we have that

$$\alpha_2' = \alpha_{2,\text{THP}} = -\,\text{Q}(s_{k_2} + l_{2,1} s_{k_1}) \tag{42}$$

and $v_2 = s_{k_2} + \hat{\alpha}_2' + l_{2,1} s_{k_1}$. If we assume that in general, for $m = 1, \ldots, j-1$ we have

$$v_m = s_{k_m} + \hat{\alpha}_m' + \sum_{i=1}^{m-1} l_{j-1,i}(s_{k_i} + \hat{\alpha}_i'), \tag{43}$$

then the expression for $\tilde{\boldsymbol{s}}_j$ becomes

$$\begin{aligned} \tilde{s}_j &= s_{k_j} - \sum_{i=1}^{j-1} l_{j,i}^{-1} v_i = \ldots \\ &= s_{k_j} - \sum_{i=1}^{j-1} \sum_{m=i}^{j-1} l_{j,m}^{-1} l_{m,i} (s_{k_i} + \hat{\alpha}_i') \\ &= s_{k_j} + \sum_{i=1}^{j-1} l_{j,i} (s_{k_i} + \hat{\alpha}_i'), \end{aligned} \tag{44}$$

where we used (41). From (44) we see that (38) and (39) are equal. Furthermore, (43) holds also for $m = j$ and the mathematical induction is complete.

REFERENCES

[1] M. Joham, W. Utschick, and J. A. Nossek, "Linear Transmit Processing in MIMO Communications Systems," *IEEE Transactions on Signal Processing*, vol. 53, no. 8, pp. 2700–2712, August 2005.

[2] R. F. H. Fischer, *Precoding and Signal Shaping for Digital Transmission*, John Wiley & Sons, 2002.

[3] G. Ginis and J. M. Cioffi, "A Multi-user Precoding Scheme achieving Crosstalk Cancellation with Application to DSL Systems," in *Proc. Asilomar Conference on Signals, Systems, and Computers*, October 2000, vol. 2, pp. 1627–1631.

[4] R. F. H. Fischer, C. Windpassinger, A. Lampe, and J. B. Huber, "MIMO Precoding for Decentralized Receivers," in *Proc. ISIT 2002*, June/July 2002, p. 496.

[5] M. Joham, J. Brehmer, and W. Utschick, "MMSE Approaches to Multiuser Spatio-Temporal Tomlinson-Harashima Precoding," in *Proc. ITG SCC'04*, January 2004, pp. 387–394.

[6] J. Liu and A. Duel-Hallen, "Tomlinson-Harashima Transmitter Precoding for Synchronous Multiuser Communications," in *Proc. CISS'03*, March 2003.

[7] L. Choi and R. D. Murch, "A Pre-BLAST-DFE Technique for the Downlink of Frequency-Selective Fading MIMO Channels," *IEEE Transactions on Communications*, vol. 52, no. 5, pp. 737–743, May 2004.

[8] C. Windpassinger, R. F. H. Fischer, T. Vencel, and J. B. Huber, "Precoding in Multiantenna and Multiuser Communications," *IEEE Transactions on Wireless Communications*, vol. 3, no. 4, pp. 1305–1316, July 2004.

[9] M. Meurer, T. Weber, and W. Qiu, "Transmit Nonlinear Zero Forcing: Energy Efficient Receiver Oriented Transmission in MIMO CDMA Mobile Radio Downlinks," in *Proc. ISSSTA 2004*, September 2004, pp. 260–269.

[10] J. Liu and W. A. Krzymień, "A Novel Nonlinear Precoding Algorithm for the Downlink of Multiple Antenna Multi-User Systems," in *Proc. VTC 2005 Spring*, May 2005.

[11] K. Kusume, M. Joham, W. Utschick, and G. Bauch, "Efficient Tomlinson-Harashima Precoding for Spatial Multiplexing on Flat MIMO Channel," in *Proc. ICC 2005*, May 2005, vol. 3, pp. 2021–2025.

[12] B. M. Hochwald, C. B. Peel, and A. L. Schwindlehurst, "A Vector-Perturbation Technique for Near-Capacity Multiantenna Multiuser Communication-Part II: Perturbation," *IEEE Trans. on Communications*, vol. 53, no. 3, pp. 537–544, March 2005.

[13] C. Windpassinger, R. F. H. Fischer, and J. B. Huber, "Lattice-Reduction-Aided Broadcast Precoding," *IEEE Trans. on Communications*, vol. 52, no. 12, pp. 2057–2060, December 2004.

[14] D. Schmidt, M. Joham, and W. Utschick, "Minimum Mean Square Error Vector Precoding," in *Proc. PIMRC 2005*, September 2005.

[15] X. Shao, J. Yuan, and P. Rapajic, "Precoder Design for MIMO Broadcast Channels," in *Proc. ICC 2005*, May 2005, vol. 2, pp. 788–794.

[16] M. Grötschel, L. Lovász, and A. Schrijver, *Geometric Algorithms and Combinatorial Optimization*, Springer, 1993.

[17] L. Babai, "On Lovasz's Lattice Reduction and the Nearest Lattice Point Approximation," *Combinatorica*, vol. 6, pp. 1–14, 1986.

[18] E. Agrell, T. Eriksson, A. Vardy, and K Zeger, "Closest Point Search in Lattices," *IEEE Trans. Inform. Theory*, vol. 48, no. 8, pp. 2201–2214, August 2002.

[19] R. F. H. Fischer and C. Windpassinger, "Real-vs. Complex-Valued Equalization in V-BLAST Systems," *IEEE Electronics Letters*, vol. 39, no. 5, pp. 470–471, March 2003.

[20] H. Yao and G. W. Wornell, "Lattice-Reduction-Aided Detectors for MIMO Communication Systems," in *Proc. Globecom'02*, Nara, Japan, November 2002, vol. 1, pp. 424–428.

[21] A. L. Lenstra, H. W. Lenstra, and L. Lovasz, "Factoring Polynomials with Rational Coefficients," *Mathematische Annalen*, vol. 261, pp. 515–534, 1982.

[22] H. Cohen, *A Course in Computational Algebraic Number Theory*, Springer Verlag, 1993.